

The cellular basis of corneal transparency: evidence for 'corneal crystallins'

James V. Jester^{1,*}, Torben Moller-Pedersen², Jiying Huang¹, Christina M. Sax³, Wm Todd Kays³,
H. Dwight Cavangh¹, W. Matthew Petroll¹ and Joram Piatigorsky³

¹Department of Ophthalmology, University of Texas Southwestern Medical Center, Dallas, Texas, USA

²Department of Ophthalmology, Aarhus University Hospital, Aarhus, Denmark

³Laboratory of Molecular and Developmental Biology, National Eye Institute, Bethesda, MD, USA

*Author for correspondence (e-mail: jester@crnjsgj.swmed.edu)

Accepted 11 December 1998; published on WWW 8 February 1999

SUMMARY

In vivo corneal light scattering measurements using a novel confocal microscope demonstrated greatly increased backscatter from corneal stromal fibrocytes (keratocytes) in opaque compared to transparent corneal tissue in both humans and rabbits. Additionally, two water-soluble proteins, transketolase (TKT) and aldehyde dehydrogenase class 1 (ALDH1), isolated from rabbit keratocytes showed unexpectedly abundant expression (~30% of the soluble protein) in transparent corneas and markedly reduced levels in opaque scleral fibroblasts or keratocytes from hazy, freeze injured regions of the cornea. Together these data suggest that the relatively high expressions of TKT

and ALDH1 contribute to corneal transparency in the rabbit at the cellular level, reminiscent of enzyme-crystallins in the lens. We also note that ALDH1 accumulates in the rabbit corneal epithelial cells, rather than ALDH3 as seen in other mammals, consistent with the taxon-specificity observed among lens enzyme-crystallins. Our results suggest that corneal cells, like lens cells, may preferentially express water-soluble proteins, often enzymes, for controlling their optical properties.

Key words: Keratocyte, Crystallin, Corneal transparency, Aldehyde dehydrogenase class 1, Transketolase

INTRODUCTION

Development of non-invasive optical imaging techniques using confocal microscopy have provided an opportunity to localize and identify light reflecting and scattering structures within the living, transparent cornea (Li et al., 1997; Moller-Pedersen et al., 1997). As expected from an optically transparent tissue, the normal cornea scatters light predominantly at the air/cornea and cornea/water interface where the change in the index of refraction of light is greatest with only minor scattering by structures inside corneal tissue, e.g. nerves and cell nuclei. By contrast, swollen or stored (Hennighausen et al., 1998; Jester et al., 1992), fixed (Jester et al., 1992), and wounded corneas (Ichijima et al., 1993; Jester et al., 1992; Moller-Pedersen et al., 1998a,b) show a decrease in corneal transparency that correlates with a dramatic increase in light scattering from corneal stromal cells (keratocytes) producing remarkably detailed images of cellular structure and organization. This cell-related loss of corneal clarity is not taken into account by the conventional model of corneal transparency based on the regular ultrastructural array of tightly packed, orthogonally arranged collagen fibers (Maurice, 1957), and suggests a novel and previously unrecognized cellular contribution to the maintenance of normal corneal transparency, similar to that proposed for the transparent cellular lens of the eye.

The optical properties of the eye lens, which has only a surrounding basement membrane as an extracellular matrix, depends upon the accumulation of soluble proteins, called

crystallins. Many crystallins of vertebrates and invertebrates are related or identical to metabolic proteins and often differ among species in a taxon-specific fashion (de Jong et al., 1989; Piatigorsky and Wistow, 1989; Tomarev and Piatigorsky, 1996; Wistow and Piatigorsky, 1988). Certain enzymes, i.e. aldehyde dehydrogenase class 3 (ALDH3) and transketolase (TKT), have also been shown to accumulate in corneal epithelia (Abedinia et al., 1990; Boesch et al., 1996; Cooper et al., 1991; Cuthbertson et al., 1992; Evces and Lindahl, 1989; Guo et al., 1997; Sax et al., 1996). By analogy with the lens enzyme-crystallins, it has been proposed that the abundant corneal enzymes have a structural function related to transparency in the epithelial cells (see Piatigorsky, 1998). However, no direct evidence has ever been obtained to support a refractive function of the abundant enzymes in either the lens or cornea. Here we provide the first evidence that two abundant enzymes, TKT and aldehyde dehydrogenase class 1 (ALDH1), may indeed contribute to cellular transparency in the rabbit cornea.

MATERIALS AND METHODS

Patients and animals

Confocal microscopic evaluations performed on human patients were conducted prior to and following excimer laser photorefractive keratectomy surgery (PRK), which was performed for the correction of near sightedness. Informed consent was obtained from all patients as part of a Phase II protocol from the Food and Drug Administration

and Institutional Review Board at the University of Texas Southwestern Medical Center at Dallas to evaluate PRK using Aesculap-Meditec Excimer Laser (MEL 60, Model 94, Heroldsberg, Germany). Human Eye Bank corneas from the University of Texas Southwestern Medical Center, Transplant Services, were obtained for light microscopic evaluation.

A total of 47 albino rabbits weighing approximately 3-4 kg were used to evaluate corneal light scattering and expression of protein by keratocytes isolated from transparent and opaque tissue. Handling and care of animals were in accordance with the Association for Research in Vision and Ophthalmology Statement for the Humane Use of Animals in Ophthalmic and Vision Research (ARVO, 1994). In a group of 5 rabbits (Group 1), corneal light scattering after excimer laser PRK was evaluated by confocal microscopy to establish the similarity between human and rabbit corneal haze following PRK. Another two groups of rabbits (Groups 2 and 3; 6 rabbits each) were used to identify the expression of proteins from isolated keratocytes. The remaining 30 rabbits were divided into one group of 10 rabbits (Group 4) and a second group of 20 rabbits (Group 5) that received freeze injuries in one eye and were evaluated by confocal microscopy according to the procedures outlined below.

Confocal microscopy and histology

Confocal microscopy was performed using a modified tandem scanning reflected-light confocal microscope (Ophthalmic Tandem Scanning Microscope, Model 165A, Tandem Scanning Corp., Reston, VA) which has a 9 μm , z-axis resolution (Petroll et al., 1993). Details concerning the use of this microscope on patients and live animals have been previously described (Li et al., 1997; Moller-Pedersen et al., 1997; Petroll et al., 1996). Three-dimensional constructs of the cornea were made by displaying a through-focus, z-series of images in a six-voxel-thick, surface projection in the 'Volume Render' tool of the Analyze Software Package (Mayo Medical Ventures, Rochester, MN). Selected 2-D and 3-D images were contrast adjusted using Adobe Photoshop Version 3.0 (Adobe Systems Inc., Mountain View, CA) and were printed using a Kodak Digital Science 8650PS printer (Kodak, Rochester, NY).

Tissue evaluated by light microscopy was fixed in 2.5% glutaraldehyde in phosphate buffer, pH 7.4. For gold chloride staining, tissue was rinsed in phosphate-buffered saline (PBS), stained in 1.0% gold chloride solution followed by immersion in acidulated water according to previously described methods (Roza and Beuerman, 1982). Gold chloride stained and unstained tissue specimens were then dehydrated in graded ethanol and embedded in glycolmethacrylate. Tissue blocks were cut using a Reichert-Jung 2050 microtome (Leica, Deerfield, IL) and sections from unstained tissue blocks stained with hematoxylin and eosin. Tissue sections were photographed using a Leica Diaplan microscope (Leica).

Quantitative measurement of backscattered light from corneas

As described recently (Li et al., 1997; Moller-Pedersen et al., 1997), a depth intensity profile of backscattered light from the cornea was obtained by focusing through the cornea using the confocal microscope set at a constant lens speed and video camera setting. Images of the through focus were captured on Super VHS videotape and the video images later digitized on a Silicon Graphics workstation (SGI, Mountain View, CA) using specially designed software. The pixel intensity of each image in the through focus was obtained by calculating the average pixel intensity in the central 180×180 pixel region ($285 \mu\text{m} \times 285 \mu\text{m}$) of each digitized image. The average intensity of each image was then plotted as a function of z-axis depth. The intensity curve (see Fig. 5B) depicts the major reflections from interfaces between adjacent sublayers in the cornea, as well as the irregular and/or elevated reflections in the stroma. The lens speed used in this experiment was 80 $\mu\text{m}/\text{second}$, and the average corresponding focal plane speed was approximately 32 $\mu\text{m}/\text{second}$. Since the video

images were captured and digitized at 30 frames/second, consecutive images were separated in the z-axis by approximately 1.06 μm .

The amount of backscattered light from the corneal stroma was quantitated by integrating the area under the curve beginning at the basal lamina peak (see Fig. 5B, bl) to just before the endothelial peak (see Fig. 5B, Endo). Using the lowest pixel intensity level detected before the basal lamina as a background pixel-intensity value, the area was calculated using the following equation:

$$\text{Area} = \sum \{ (I_i + I_{i+1})/2 - I_{\text{BK}} \} \Delta z_i ;$$

$$\Delta z_i = z_i - z_{i-1} ;$$

where I_i is the intensity value of image i ; I_{BK} is the background intensity before the basal lamina; z_i and z_{i-1} are the focal plane positions of image i and $i-1$. The unit of measurement (U) is defined as $\mu\text{m} \times \text{pixel intensity}$.

Rabbit eye injuries

Excimer laser PRK was performed on one eye of 5 anesthetized rabbits from Group using techniques previously published (Moller-Pedersen et al., 1998a,b). Animals were anesthetized with 30 mg/kg ketamine hydrochloride and 3 mg/kg xylazine and photoablations, 6 mm diameter and 90 μm deep, made using an Aesculap-Meditec Excimer Laser (MEL 60, Model 94, Heroldsberg, Germany). Wound healing responses were followed by confocal microscopy. Standard, 6 mm diameter, central transcorneal freeze injuries were performed on one eye each of anesthetized rabbits from Group 4 and Group 5 according to techniques previously described (Ichijima et al., 1993). Eyes were evaluated at day 7 and 14 after injury by confocal microscopy and rabbits sacrificed at day 14 by the intravenous injection of sodium pentobarbital (100 mg/kg). In rabbits from Group 4 (10 rabbits), both eyes (wounded and contralateral control) were enucleated at the time of sacrifice, the corneas removed and the keratocytes isolated from the hazy/opaque, freeze-wounded corneas, and compared to the contralateral clear, transparent corneas. In rabbits from Group 5 (20 rabbits), eyes were enucleated and the corneas removed at the time of sacrifice. Keratocytes were then isolated from a central, hazy/opaque portion of the wounded cornea by cutting a 6 mm diameter corneal button using a trephine. Keratocytes residing in the transparent corneal rim adjacent to the hazy/opaque corneal tissue in eyes from Group 5 animals were also isolated and the proteins compared to keratocytes isolated from the hazy/opaque portion of wounded corneas in the same eyes and the normal corneas obtained from the contralateral eyes.

Isolation and characterization of keratocyte proteins

Normal rabbit eyes were obtained either fresh from Group 2 and 3 immediately after sacrifice or shipped to the laboratory on ice in MEM medium within 24 hours after death from an abattoir (Pel Freez, Rogers, AK). Freeze injured rabbit eyes from Groups 4 and 5 were obtained immediately after sacrifice. Keratocytes were isolated from the corneal tissue by first removing the surface epithelium from the cornea by scraping with a scalpel blade and wiping the surface with alcohol. The cornea, normal or freeze injured, was then removed, 1 mm anterior to the limbus, and the endothelium removed with a cotton tipped applicator. For freeze injured corneas from Group 5, the hazy/opaque tissue was isolated by cutting a 6 mm, central corneal button using a 6 mm diameter corneal trephine, which removed the area of freeze injury. To collect opaque, scleral cells, the overlying conjunctiva, comprising loose connective tissue, was dissected from the sclera, which is composed of dense connective tissue, from eyes obtained from Groups 2 and 3. Additionally, the retina and underlying choroid was removed by scraping with a scalpel blade. The tissue (sclera and cornea) was then digested for 4 hours in sterile 2.0 mg/ml collagenase (Gibco-BRL, Gaithersburg, MD) and 0.5 mg/ml hyaluronidase (Worthington, Freehold, NJ) in MEM (Gibco-BRL) at 37°C. This digestion protocol is routinely used to isolate a pure

population of keratocytes for culture without contamination from corneal epithelium and endothelium. The scleral cells obtained using this technique are comprised predominantly of scleral fibroblasts with some contaminating vascular cells.

Keratocytes and scleral cells released from the tissues obtained from the various groups were then centrifuged, washed twice in PBS and either placed in buffer (25 mM Tris-HCl, pH 7.4, with 1 mM EDTA, 1 mM EGTA, 10 mM dithiothreitol, 5 µg/ml antipain, 5 µg/ml pepstatin A, and 1 mM phenylmethylsulfonyl fluoride) containing 1% SDS (total protein) or sonicated in 1 ml of buffer alone and separated into water-soluble and insoluble fractions before addition of final buffer containing 1% SDS. Samples were then examined on 10% SDS-polyacrylamide gels and stained with Coomassie blue. For peptide sequence analysis, the Coomassie blue stained protein bands were excised and subjected to treatment with trypsin according to previously described methods (Kurzchalia et al., 1992). For immunoblotting, proteins from SDS-PAGE were transferred to nitrocellulose membranes and reacted with rabbit anti-mouse TKT antibodies previously shown to recognize mouse corneal epithelial TKT (Sax et al., 1996) and a rabbit anti-human ALDH1 (gift from Dr R. Lindahl, Department of Biochemistry, University of South Dakota, Vermillion, SD).

Generation of cDNA probes

ALDH

Rabbit corneal mRNA was used as a template for RT-PCR reactions to produce cDNA products for ALDH1, ALDH2 and ALDH3. Primers used to generate RT-PCR products included: (1) Human ALDH1 sequence +32 to +55 (5'-3') CGT TGG TTA TGC TCA TTT GGA AGA and +776 to +753 (3'-5') CTT TTG ATC ACG TCA TCT AAA GAT oligonucleotides to generate a 745 bp product. (2) Human ALDH2 sequence +209 to +232 (5'-3') CGC TCC TGA TGC AAG CAT GGA AGC and +953 to 930 (3'-5') CTC CCA ACA ACC TCC TCT ATG GCT oligonucleotides to generate a 745 bp product. (3) Mouse ALDH3 using +4 to +27 (5'-3') CCA GGA GTT CCA GCT GCT GGA GAG and +468 to +445 (3'-5') TTC CGA GGG CTT GAG GAC CAC GGC oligonucleotides to generate a 457 bp cDNA product. cDNA products were cloned into pCR II-TOPO and sequenced to confirm identities and the cDNA used in northern blot analyses.

TKT

Because the mouse TKT cDNAs developed by Sax et al. (1996) do not cross-hybridize well with rabbit mRNAs on northern blots, rabbit cDNA probes were needed. To accomplish this goal, RT-PCR primers were designed against regions of the TKT gene in which the mouse and human sequences exhibited 100% identity. The RT primer (5'GGTCATCCTTGCTCTTCAGG3') corresponded to base pairs 1595 to 1576 of the mouse TKT cDNA (GenBank #U05809). The sense PCR amplification primer (5'GGACAAGATAGCCACC-CGGA3') corresponded to base pairs 1027 to 1046 in the mouse TKT cDNA (GenBank #U05809). Using total RNA isolated from rabbit corneal epithelial cells, rabbit corneal keratocytes and whole mouse cornea, 539 bp cDNA products were obtained, cloned into the pCR II-TOPO vector (Invitrogen), and sequenced to confirm identities before use in northern blots.

Northern blotting

RNA was extracted from rabbit corneal epithelial cells and keratocytes and whole mouse cornea using the RNazol method (TRI reagent; Molecular Research Center, Inc., Cincinnati, OH). Rabbit corneas were obtained from an abattoir and mouse corneas were from 3-6 month old animals; batches of 50 corneas were extracted at a time with 2-3 µg of total RNA being obtained per cornea. The RNA was electrophoresed (10 µg/lane) through an agarose/formaldehyde gel, blotted overnight in 20× SSC, rinsed in 2× SSC, UV-crosslinked and air dried. The blots were prehybridized for 2 hours at 65°C and then

hybridized overnight at 65°C with the cloned cDNA probes derived by RT-PCR of ALDH1, ALDH2, ALDH3 and TKT mRNAs. Blots were then rinsed in 2× SSC at room temperature, followed by consecutive rinses of 6× SSC in 0.1% SDS at 65°C, 2× SSC in 0.1% SDS at 65°C, and 2× SSC at room temperature.

RESULTS

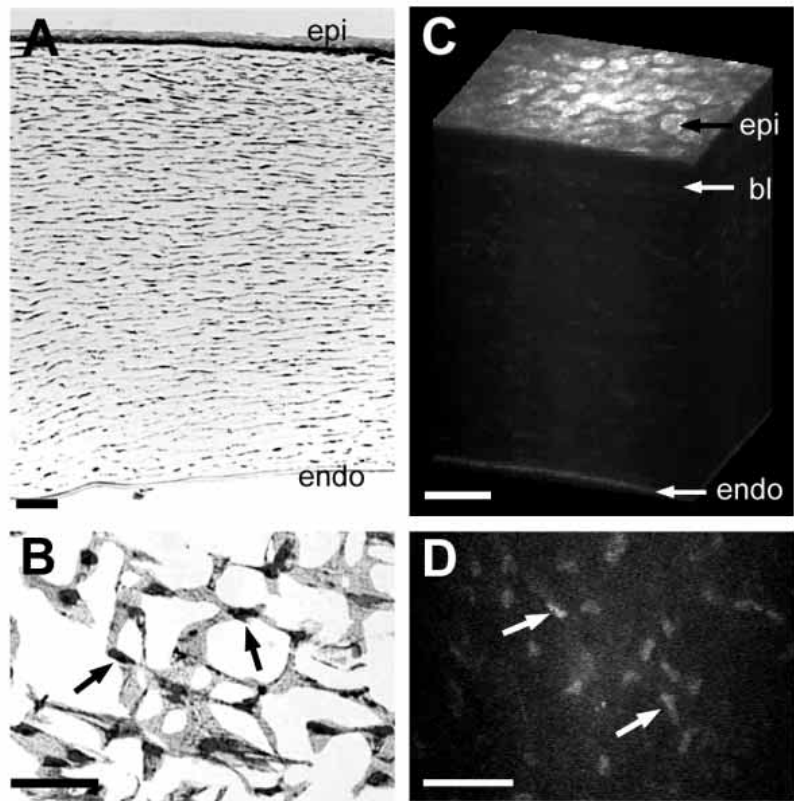
Morphologic appearance of the corneal keratocytes

Histologic sections from Human Eye Bank corneas showed that the cornea was approximately 500-750 µm thick and comprised of a multicellular, anterior epithelial layer and a monocellular, posterior endothelial layer that was separated by a compact, fibrous connective tissue or stroma (Fig. 1A). The corneal stroma comprised ~90% of the corneal thickness and contained corneal fibrocytes (keratocytes) interspersed between prominent collagen bundles. When the Human Eye Bank corneas were sectioned tangential to the epithelial surface, keratocytes (Fig. 1B, arrows) appeared as very large (2,000 µm²), flat cells that had long, broad, interconnecting processes which extended to adjacent keratocytes (Jester et al., 1994; Watsky, 1995). Overall the keratocytes have been shown to comprise from 10% to 40% of the corneal volume dependent on age (Kaye, 1969).

Using reflected light confocal microscopy, which collects backscattered or reflected light, reconstructing the living cornea from patients prior to surgery showed two major light reflecting structures located at the anterior and posterior corneal surfaces corresponding to the anterior surface epithelium and posterior endothelial layer (Fig. 1C, epi and endo, respectively). In the transparent corneal stroma, the principal structure that reflected light was the nuclei of corneal keratocytes (Fig. 1D, arrows). When confocal microscopic images from patients before surgery (Fig. 1D) were compared to the tangential histologic sections of the corneal stroma from Eye Bank corneas (Fig. 1B), it was apparent that the cell body of the corneal keratocyte was invisible and did not produce significant backscattering of light under normal, transparent conditions.

Interestingly, patient corneas after excimer laser photorefractive surgery, where the anterior surface of the cornea was removed by tissue photoablation, developed opaque or 'hazy' regions months after surgery (Fig. 2A). Using confocal microscopy, the areas of corneal haze appeared to correlate with a marked increase in the backscattered light from what appeared to be keratocytes, which revealed in remarkable detail the keratocyte organization within the tissue (Fig. 2B). In order to identify the origin of corneal haze more clearly, we used a rabbit model of PRK that shows a similar pattern of corneal haze following PRK as that observed in patients (Moller-Pedersen et al., 1998a,b). Interestingly, in rabbits from Group 1, backscattering of light by migrating keratocytes (Fig. 2C) and corneal myofibroblasts (Fig. 2D) was shown to be the principle source of corneal haze after surgery confirming earlier reports (Chew et al., 1995; Moller-Pedersen et al., 1998a,b). In other detailed confocal microscopic and correlative histopathologic studies, enhanced backscattering of spindle shaped, migrating keratocytes and myofibroblasts have been identified in rabbit eyes following freeze injury

Fig. 1. Normal human cornea. (A) Conventional light micrograph of fixed, gold chloride stained Human Eye Bank cornea cut in cross section showing the corneal epithelium (epi) and endothelium (endo) separated by corneal stroma. (B) Light micrograph of gold chloride stained tissue cut parallel to the surface of the cornea showing stromal keratocytes (arrows). (C) 3-Dimensional display of a patient cornea prior to PRK surgery constructed from a through-focus series of 2-dimensional, in vivo reflected light, confocal microscopic images taken from the anterior to posterior cornea, z-axis. Note that the major light scattering structures in the living cornea are the corneal surface epithelium (epi), the basal lamina (bl) and the corneal endothelium (endo). (D) 2-Dimensional, in vivo CM image taken from the stromal region of the through-focus, z-series shown in C. Note that only the nuclei of the keratocytes show scattering of light and that the organization and morphology of the nuclei is similar to that shown in the tissue section (see B). No scattering was detected from the keratocyte cell body. Bars, 100 μ m.



(Ichijima et al., 1993) and full-thickness penetrating injury to the cornea (Jester et al., 1995).

Identification of keratocyte TKT and ALDH1

To further explore differences between fibroblasts from transparent and opaque tissue, protein extracts from total (lane 1), water-soluble (lane 2) and insoluble (lane 3) keratocyte fractions obtained from rabbits in Group 2 were examined by SDS-PAGE (Fig. 3A) and compared to fibroblasts from opaque, scleral, tissue (Fig. 3B). Two prominent proteins with apparent molecular masses of approximately 70 kDa and 54 kDa were identified (arrowheads) in the soluble protein fraction (Fig. 3A, lane 2 and Fig. 3B, lane 1). These bands were

absent from the water-insoluble cell fraction (Fig. 3A, lane 3), and were markedly reduced in the water-soluble protein extracts of cells from opaque scleral tissues (Fig. 3B, lane 2). Based on densitometry from five separate experimental samples (control eyes from Groups 2, 4, and 5 and two separate samples of 40 eyes each obtained from the abattoir), these proteins individually comprised $13.2 \pm 3.4\%$ (11.0% to 17.7% for the ~70 kDa protein) and $14.7 \pm 3.4\%$ (10.0% to 18.1% for the 54 kDa protein) of the water-soluble proteins of the corneal keratocytes, giving a combined total of $27.9 \pm 5.4\%$ (21.0% to 35.8%).

The primary structure of selected tryptic peptides derived from these bands showed sequence homology to mouse and

Fig. 2. Human patient (A and B) and rabbit (C and D) corneas following excimer laser photorefractive keratectomy (PRK). (A) Clinical biomicrograph of patients cornea showing presence of central corneal sub-epithelial haze. (B) 2-Dimensional in vivo CM micrograph showing broadly thickened and distinct keratocyte cell bodies in the region of corneal haze. (C) Cornea from a rabbit in Group 1, 7 days after PRK surgery showing spindle shaped migratory keratocytes. (D) Same rabbit cornea, 21 days after PRK showing the presence of myofibroblasts forming a broad, interconnected meshwork of cells within a region of corneal fibrosis. Bar, 100 μ m.

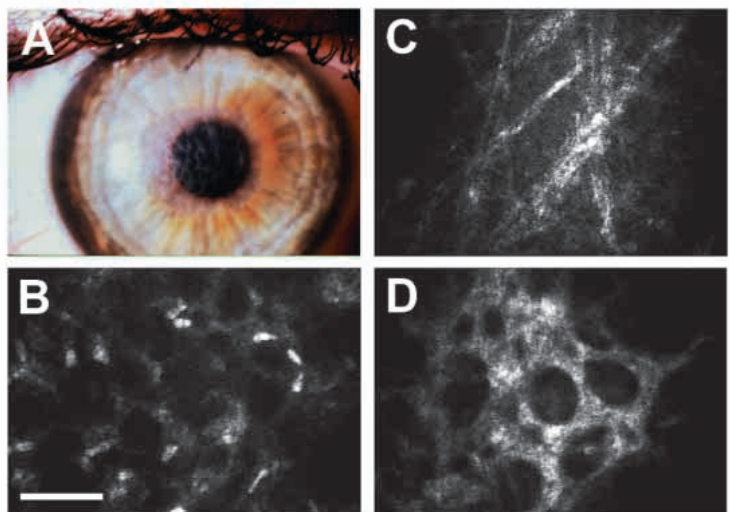


Table 1. Tryptic peptide amino acid sequence analysis of soluble keratocyte proteins

| ~70 kDa protein | | | 54 kDa Protein | | |
|-----------------|----------|-------------------|----------------|----------|---------------------------------|
| Source | Sequence | Amino acid | Source | Sequence | Amino acid |
| Peptide A | | N R T F D L F K | Peptide A | | L L Y K |
| mTKT* | 344-352 | N S T F S E L F K | hALDH-1‡ | 88-91 | L L Y K |
| hTKT§ | 344-352 | N S T F S E T F K | | | |
| Peptide B | | E F K P A E L L R | Peptide B | | G Y F I Q P T V F S N V T G E M |
| mTKT | 595-603 | S G K P A E L L K | hALDH-1 | 379-394 | G Y F V Q P T V F S N V T D E M |
| hTKT | 595-603 | S G K P A E L L K | | | |
| Peptide C | | S F D Q I R | Peptide C | | I F V E E S I Y D E |
| mTKT | 396-402 | A F D Q I R | hALDH-1 | 309-318 | I F V E E S I Y D E |
| hTKT | 396-402 | A F D Q I R | | | |

*Mouse transketolase.
‡Human aldehyde dehydrogenase class 1.
§Human transketolase.

human TKT for the ~70 kDa protein and human ALDH1 for the 54 kDa protein (Table 1). Reaction of protein samples with a mouse anti-TKT monoclonal antibody (Sax et al., 1996) in immunoblots confirmed that the ~70 kDa protein was TKT (Fig. 3B, lane 3) and that the expression of TKT in scleral fibroblasts was greatly reduced (Fig. 3B, lane 4). Similarly, reaction of water-soluble proteins with rabbit antibodies to human ALDH1 showed intense staining of the 54 kDa protein in extracts from rabbit keratocytes (Fig. 3B, lane 5) while extracts from scleral fibroblasts was markedly reduced (Fig. 3B, lane 6). Staining of gels with antibodies to actin, showed comparable intensities for both corneal keratocytes and scleral cells indicating similar loads (data not shown).

Northern blot analysis was performed to examine the relative amounts of ALDH1, ALDH2, ALDH3 and TKT mRNAs in the epithelial cells and keratocytes of the normal rabbit cornea obtained from an abattoir. RNA from whole corneas of adult

mice were included in these tests to provide a positive control for our observation that rabbits differ from other mammals, including mice (See Piatigorsky, 1998 for review), by accumulating principally ALDH1 rather than ALDH3 in their corneal epithelial cells. Previous histochemical experiments established that high expression of ALDH3 occurs in the epithelial cells and not in the keratocytes of the mouse cornea (Kays and Piatigorsky, 1997), obviating the need to separate epithelial cells from keratocytes in these experiments. Significant TKT expression is found in both the epithelial cells (Sax et al., 1996) and keratocytes of the mouse cornea (Guo et al., 1997). The present northern blots showed that both epithelial cells and keratocytes of rabbit corneas had abundant ALDH1 mRNA (Fig. 4, lanes 2 and 3, respectively) and negligible amounts of ALDH3 mRNA (Fig. 4, lanes 5 and 6, respectively). As expected (Kays and Piatigorsky, 1997), the mouse cornea has predominantly ALDH3 mRNA (Fig. 4, lane

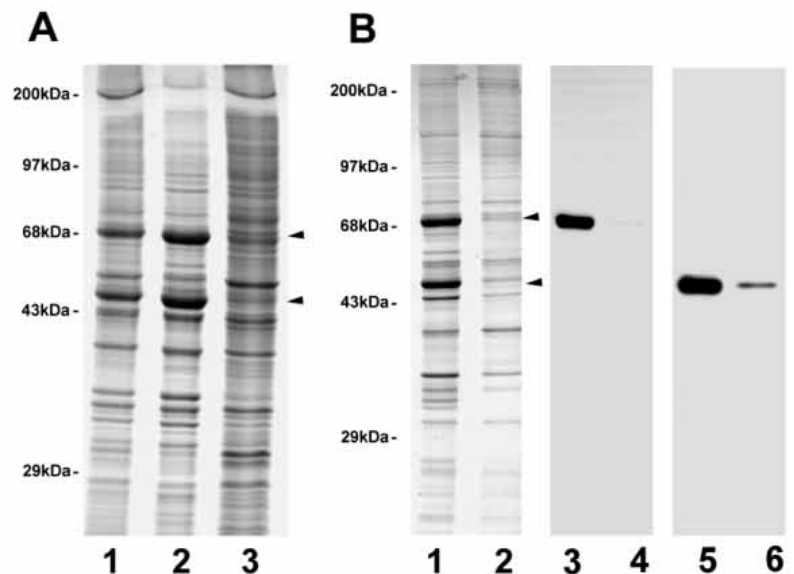


Fig. 3. Identification of water-soluble proteins. (A) Coomassie-blue stained SDS-PAGE of total (lane 1), soluble (lane 2), and insoluble (lane 3) cellular proteins from keratocytes obtained from transparent corneas from rabbits in Group 2. Note the presence of two prominent bands (arrows) in the soluble fraction. (B) SDS-PAGE and immunoblot of water-soluble proteins extracted from normal keratocytes (lane 1, 3, and 5) and opaque scleral fibroblasts (lane 2, 4, and 6). High expression of TKT (lanes 3 and 4) and ALDH1 (lanes 5 and 6) are noted in keratocytes (lanes 3 and 5) but not scleral cells (lanes 4 and 6).

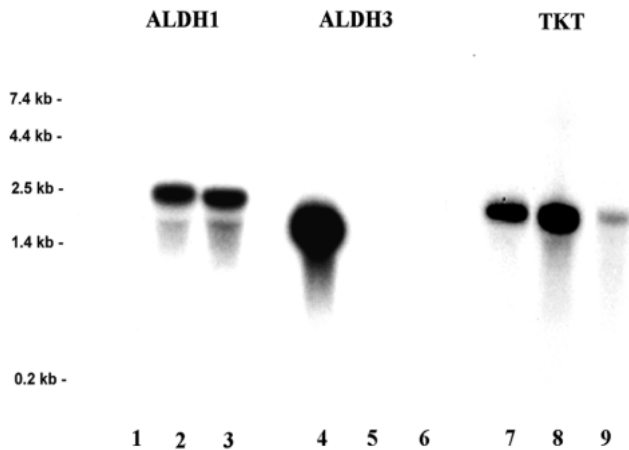


Fig. 4. Northern blots of total RNA (10 µg) extracted from mouse cornea (lanes 1, 4, 7), compared to corneal epithelium (lanes 2, 5, 8) and rabbit corneal keratocytes (lanes 3, 6, 9) from rabbits eyes obtained from an abattoir. RNA was probed with cDNA products specific for ALDH1 (lanes 1-3), ALDH3 (lanes 4-6) and TKT (lanes 7-9).

4) with little if any detectable ALDH1 mRNA (Fig. 4, lane 1). No hybridization signal was obtained for ALDH2 in the present tests (data not shown). TKT mRNA was found in both the mouse (Fig. 4, lane 7) and rabbit (Fig. 4, lanes 8 and 9) corneas, with at least three times more in the epithelium (lane 8) than in the keratocytes (lane 9) of the rabbit cornea. A similar result was obtained in an independent test conducted with a different preparation of rabbit corneal epithelial cell cells and keratocytes (data not shown).

Modulation of TKT and ALDH1 expression in repopulating keratocytes

In order to evaluate the expression of these water-soluble proteins in opaque corneal keratocytes, we characterized highly reflective corneal keratocytes from opaque corneas 2 weeks after freeze injury of rabbits from Groups 4 and 5. Using freeze injury was more advantageous than PRK since the former is a full-thickness corneal injury resulting in repopulation of the entire acellular corneal tissue (Ichijima et al., 1993). Isolation of the opaque region of the cornea would therefore ensure collection of predominantly migrating cells with few normal, transparent keratocytes. PRK, on the other hand, only effects the superficial keratocytes (Moller-Pedersen et al., 1998a,b) to a depth of 100 µm. Isolation of the cornea underlying the region of the PRK would result in collection of migrating keratocytes in the anterior 1/3 and normal keratocytes in the remaining 2/3 of the cornea making detection of any change in protein expression more difficult.

Evaluation of corneas from rabbits in Group 4 by confocal microscopy at 7 and 14 days after injury confirmed earlier findings and showed prominent backscattering of light in the anterior portion of the cornea (Fig. 5A). The image intensity depth profile (Fig. 5B), which provides an estimate of the intensity of backscattered light, showed a markedly elevated profile within the corneal stroma that equalled 7186 U (pixel*µm) compared to 88 U in the transparent cornea immediately adjacent to wounded cornea in the same eye. Although freezing results in immediate swelling of the cornea,

it should be noted that the thickness of the cornea returns to normal by 7 days after injury as shown by the coincident epithelial and endothelial peaks for both the transparent and hazy portions of the same cornea (Fig. 5B), consistent with earlier observations (Ichijima et al., 1993). This finding indicates that backscattering of light was not related to increased corneal hydration (swelling) causing increased separation of the collagen fibers at 7 days or later.

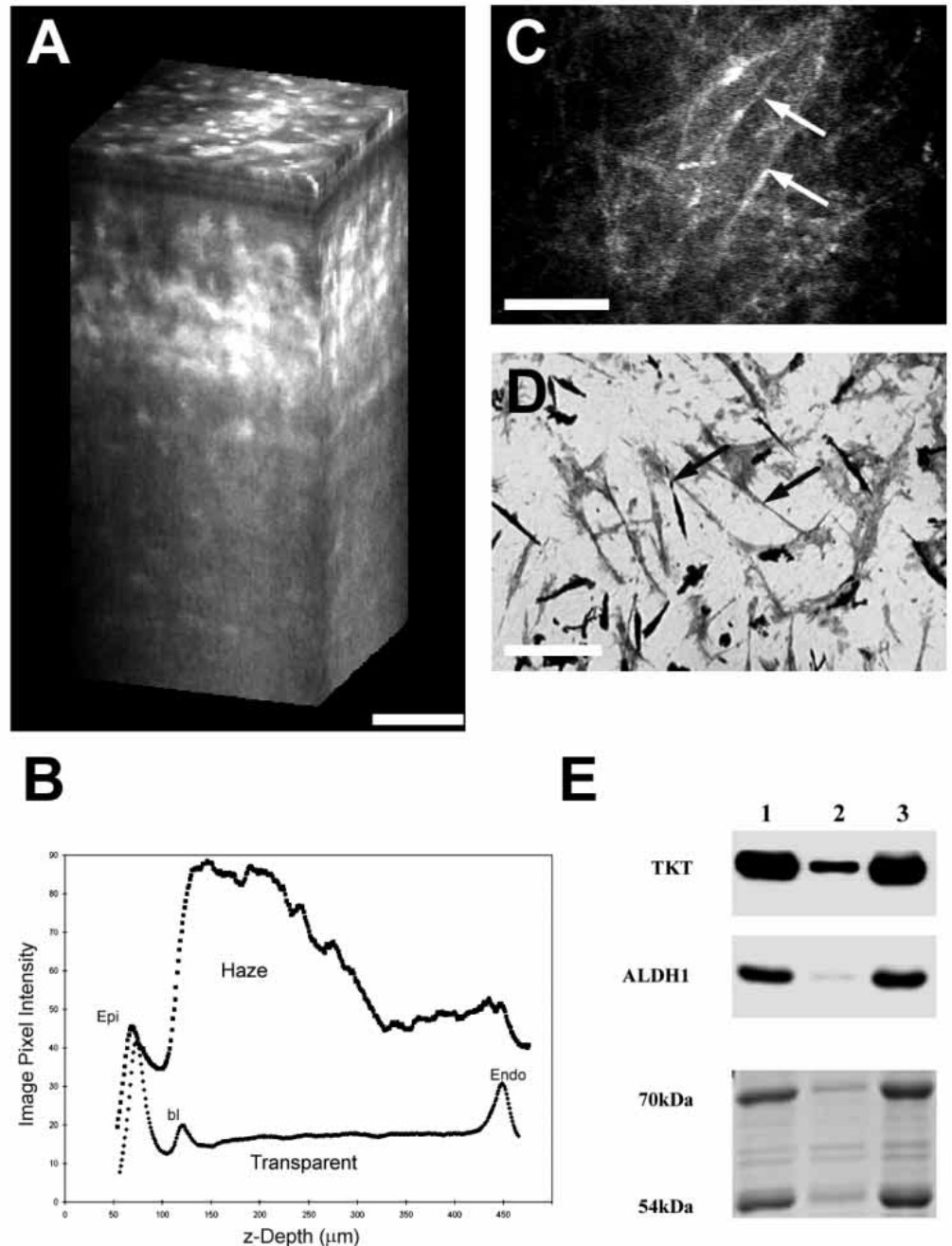
Examination of the 2-dimensional images showed the backscattered light to be localized to spindle shaped structures (Fig. 5C) that histologically correlated with the presence of intact, migrating keratocytes (Fig. 5D). The fact that these structures represented migrating and not dead fibroblasts was supported by the finding that they first appeared in the peripheral cornea, immediately adjacent to the area of injury 3 days after freezing. Additionally, these structures appeared more centrally by day 7 and completely repopulated the cornea by day 14 suggesting cell migration.

Comparison of soluble proteins from transparent keratocytes isolated from the contralateral eye (Fig. 5E, lane 1) or transparent cornea adjacent to the wound obtained from rabbits in Group 5 (Fig. 5E, lane 3) to migrating keratocytes within the wound (lane 2) showed a marked decrease in the Coomassie blue staining of the ~70 kDa/TKT and 54 kDa/ALDH1 proteins from migrating keratocytes. Averaging the results from the two duplicate experiments from Group 4 and Group 5 and comparing the density of the 70/54 kDa proteins to the earlier findings for normal keratocytes showed a significant 50% decrease ($P < 0.025$) in the apparent amount of these two water-soluble proteins in migrating keratocytes. Immunoblots using antibodies against TKT and ALDH1 confirmed the marked decrease of TKT and ALDH1 in the reflective keratocytes. Overall, the expression of ALDH1 and TKT in the rabbit keratocyte was high (~30% of soluble proteins) in normal keratocytes which did not scatter light and was significantly decreased a minimum of 50% in highly reflective keratocytes.

DISCUSSION

Previous studies on corneal transparency have focussed on the extracellular stromal matrix. Maurice (1957) proposed that the uniformity of collagen size and organization gives rise to destructive interference of the scattered light between the fibers that limits the intensity of the scattered light passing through the cornea. Goldman and Benedek (1967) modified this view by proposing that the periodic fluctuation in the index of refraction is the fundamental mechanism explaining light scattering. They suggested that light scattering is dependent on the wavelength of incident light and the distance separating fluctuations in refractive index and/or the magnitude of the refractive index fluctuation. While the normal cornea transmits >90% of the incident light, the stroma accounts for 75% of the light that is scattered at angles above 30° (Farrell and McCally, 1976; McCally and Farrell, 1976), with collagen fibers being the primary scatterers based on mathematical models (Freund et al., 1986). However, it has also been noted that the corneal keratocytes contribute to specular or backward scattered light and are the major source of scattering at small angles (Andreo and Farrell, 1982; Gallagher and Maurice, 1977; McCally and

Fig. 5. Transcorneal freeze injury in the rabbit. (A) 3-Dimensional display of the living cornea 14 days after injury showing greatly enhanced scattering of light from the anterior cornea from rabbits in Group 4. (B) Image intensity depth profile from cornea shown in 'A' within region of freeze injury (Haze) compared to transparent cornea (Transparent) adjacent to the freeze injury in the same cornea (curves have been off-set along the y-axis to better demonstrate differences). Note the presence at baseline of peak intensities localized to the epithelial surface (Epi), basal lamina (bl) and endothelium (Endo). (C) 2-Dimensional in vivo CM image taken from the 3-dimensional stack shown in A. Note that the backscattering of light shown in A is from the highly reflective, spindle shaped structures. (D) Light micrograph of gold chloride stained tissue showing that migrating keratocytes assume a spindle shape morphology similar to that detected by in vivo CM and shown in C. (E) SDS-PAGE and immunoblots of water-soluble proteins extracted from keratocytes isolated from normal cornea (lane 1), wounded cornea (lane 2) and the corneal rim adjacent to the wound cornea (lane 3) from rabbits in Group 5. Note the marked reduction in the ~70 kDa and 54 kDa proteins in the injured keratocytes (lane 2) and the decreased staining with antibodies to TKT and ALDH1, while there is no change in the staining of keratocytes isolated from the adjacent corneal rim (lane 3). Bars, 100 μ m.



Farrell, 1982). Our present in vivo confocal microscopy results suggest that the keratocyte nuclei are a major source of this backscattering of light and show that migrating cells in a wounded cornea are much more reflective than their stationary counterparts in a normal, transparent cornea.

Presumably the nuclear light scattering that we have observed in the keratocytes of the transparent cornea is due to inhomogeneities in the refractive index of the nucleus which has a cross-sectional thickness of 1 to 2 μ m (Muller et al., 1995). Of particular interest, however, is the fact that the large dendritic cellular processes of normal keratocytes, which have a thickness ranging from 0.2 to 0.9 μ m (Muller et al., 1995), show negligible backscattering of light even using high resolution laser scanning confocal microscopy (Hennighausen

et al., 1998). We propose that the relatively high concentrations of ALDH1 and TKT (25-30% of the soluble protein of the cell) found here in the normal rabbit keratocytes minimize the refractive index inhomogeneities in the keratocyte cytoplasm, resulting in transparency. Conversely, we propose that the selective losses of ALDH1 and TKT in migrating keratocytes contribute to their increased reflectivity by increasing the magnitude of refractive index fluctuation within the cytoplasm and/or between the cytoplasm and the extracellular environment. In short, by analogy with transparency in the cellular lens (Benedek, 1971; Bettelheim and Siew, 1983; Delaye and Tardieu, 1983), we suggest that ALDH1 and TKT act as corneal enzyme-crystallins (see Piatigorsky, 1998) in the rabbit keratocytes. Crystallins contribute to the transparent and

refractive properties of the lens by accumulating to high concentrations and minimizing the refractive index fluctuations by short range interactions within the cytoplasm of the cells (Benedek, 1983; Bettelheim, 1985).

Disrupting the normal continuities of refractive index within the cornea leads to backscattering of light by keratocytes in a manner that is consistent with the idea that ALDH1 and TKT play a role in the transparency of rabbit corneal keratocytes by functioning as enzyme-crystallins. First, there is a marked increase in the backscattering of light from keratocytes following glutaraldehyde fixation of the cornea, which does not alter the cross-sectional distances between corneal structures (Jester et al., 1992). This may be explained by the precipitation of soluble proteins in the keratocytes, which would result in a change in the relative refractive index between the keratocyte and the extracellular milieu. If this interpretation is correct it follows that the extent of reflectivity of the normal keratocyte within the stroma depends on the refractive index of its cytoplasm as determined by the levels of soluble proteins. Secondly, corneal opacification by swelling is associated with a marked increase in light scattering by keratocytes (Hennighausen et al., 1998; Jester et al., 1992). This is associated with an increase in the interfibrillar collagen spacing and the formation of water 'lakes' between collagen fibers, collagen lamellae and keratocytes (Goldman et al., 1968; Goldman and Kuwabara, 1968). It is likely that these lakes contribute to corneal opacification by increasing the distance between structures with differing refractive index and contribute to keratocyte reflectivity by increasing the magnitude of the refractive index fluctuations between the cell and its milieu due to the low refractive index of the lakes. The latter again points to the critical importance of minimizing the refractive index fluctuations between cytoplasm and environment for cellular transparency. Finally, during wound healing, increased backscattering of light by migrating keratocytes as shown in the present study or by myofibroblasts (Moller-Pedersen et al., 1998a,b) persists after the cornea has regained normal thickness and hydration. Our data are consistent with the idea that it takes some time for the migrating rabbit keratocytes to readjust their ALDH1 and TKT concentrations to become compatible with the extracellular environment and achieve cellular transparency. It is likely, of course, that the refractive index of the stroma is also changing in the healing cornea. For example, fibronectin and hyaluronic acid, which is hygroscopic, are deposited at the cell surface during cell migration (Fitzsimmons et al., 1992; Weber et al., 1997). Thus, while none of the above arguments establish that keratocyte transparency depends on regulating the levels of selected soluble proteins within the cytoplasm, the data are consistent with this idea.

A metabolic role for abundant corneal enzymes is commonly accepted. ALDH3 has been implicated in maintaining the oxidation-reduction balance of the cornea, and it has been proposed that ALDH3 protects the corneal cells against lipid peroxidation and free radical formation (Evces and Lindahl, 1989; Knoishi and Mimura, 1992; Lindahl and Peterson, 1991; Messiha and Price, 1983; Uma et al., 1996). ALDH3 may also protect against oxidative damage by absorbing UV-B irradiation (290-320 nm) (Abedinia et al., 1990; Algar et al., 1990), and it has been proposed that the major water-soluble proteins of the bovine cornea be called absorbins (Mitchell and

Cenedella, 1995). Similarly, TKT may also contribute to the reducing environment of corneal cells and protect against free radicals (Guo et al., 1997; Sax et al., 1996).

The possibility that the accumulation of soluble proteins have structural, crystallin-like roles in the cornea has been proposed earlier (Cooper et al., 1991; Cuthbertson et al., 1992; Piatigorsky, 1998; Sax et al., 1996). Historically, ALDH3 was first noted as a specific antigen in the bovine cornea (called BCP 54) comprising 20-40% of the water-soluble protein (Alexander et al., 1981; Holt and Kinoshita, 1973); later BCP 54 was shown to be ALDH3 (Abedinia et al., 1990; Verhagen et al., 1991). The high expression of BCP 54/ALDH3 in the cornea led investigators to speculate that it might contribute to transparency (Silverman et al., 1981), and indeed the name transparentin was used (Rabaey and Segers, 1981), suggesting that the cornea, like the lens, may contain crystallins. Studies have shown that BCP 54/ALDH3 is present in several mammals, but not in non-mammalian species (Cuthbertson et al., 1992; Silverman et al., 1981), indicating that corneal enzyme-crystallins may be taxon-specific, as are lens enzyme-crystallins (Piatigorsky, 1998; Wistow and Piatigorsky, 1988). Here we provide evidence that ALDH1 and TKT contribute to transparency of the keratocytes within the stroma by minimizing spatial fluctuations in refractive index, consistent with the idea that lens and cornea use common mechanisms, including gene sharing, for achieving their optical properties (Piatigorsky, 1998).

While ALDH3 is abundantly expressed in the corneal epithelial cells of numerous mammals (Abedinia et al., 1990; Cuthbertson et al., 1992; Kays and Piatigorsky, 1997; Piatigorsky, 1998), the present results show that ALDH1 is the major isomer of this enzyme present in the epithelial cells and keratocytes of the rabbit cornea. The reasons for accumulation of ALDH1 rather than ALDH3 in the rabbit cornea are not known. Recently it has been shown that ALDH1 is expressed quite highly in the human cornea, although it is present at a significantly lower concentration than ALDH3 (King and Holmes, 1998). It is noteworthy that two species of fish (chain pickerel and redhorse) have ALDH1 but not ALDH3 activity in their corneas, but the relative amount of ALDH1 with respect to the total soluble protein in these corneas is not known (Cooper et al., 1992). Only ALDH1 has been found to be a crystallin in the lens. ALDH1/ η -crystallin comprises 25% of the water-soluble lens proteins of elephant shrews (Wistow and Kin, 1991). In addition, an ALDH more closely related to ALDH1 and ALDH2 than to ALDH3 accumulates to crystallin concentrations in the lenses of cephalopod eyes (Ω -crystallin; Zinovieva et al., 1993) and of octopus light organs (L-crystallin; Montgomery and McFall-Ngai, 1992). ALDH1/ η -crystallin possesses retinaldehyde dehydrogenase activity (Graham et al., 1996); however, tests with lens extracts indicated that omega-crystallin (Zinovieva et al., 1993) and L-crystallin (Montgomery and McFall-Ngai, 1992) are enzymatically inactive (see Tomarev and Piatigorsky, 1996, for review on invertebrate crystallins).

In conclusion, we have identified a high level of cytosolic expression of ALDH1 and TKT in the keratocytes of the rabbit cornea. The specific decrease in the amounts of these proteins in highly reflective keratocytes after injury suggests that they contribute to a previously unrecognized cellular component of corneal transparency. These findings extend the concept of

enzyme-crystallins and transparency for the lens to the corneal keratocytes (Piatigorsky, 1998). A cellular component of corneal transparency may underlie transient changes in corneal clarity that occur following swelling, increased intraocular pressure and wound healing that have not been adequately addressed by x-ray diffraction models of collagen fibrillar size and spacing.

We thank Russell L. McCally, Ph.D. of the Johns Hopkins University Applied Physics laboratory for his critical comments and guidance on the physical basis of corneal transparency. Supported in part by EY07348, and Senior Scientist Awards (J.V.J.) and an Unrestricted Grant from Research to Prevent Blindness, Inc., New York.

REFERENCES

- Abedinia, M., Pain, T., Algar, E. M. and Holmes, R. S.** (1990). Bovine corneal aldehyde dehydrogenase: the major soluble corneal protein with a possible dual protective role for the eye. *Exp. Eye Res.* **51**, 419-426.
- Alexander, R. J., Silverman, B. and Henley, W. L.** (1981). Isolation and characterization of BCP 54, the major water soluble protein of bovine cornea. *Exp. Eye Res.* **32**, 205-216.
- Algar, E. M., Abedinia, M., VandeBerg, J. L. and Holmes, R. S.** (1990). Purification and properties of baboon corneal aldehyde dehydrogenase. Proposed UVR protective role. In *Enzymology and Molecular Biology of Carbonyl Metabolism*, vol. 284 (ed. H. Wiener and D. W. Crabb), pp. 53-60. Plenum Press, New York.
- Andreo, R. H. and Farrell, R. A.** (1982). Corneal small-angle light-scattering theory: wavy fibril models. *J. Opth. Soc. Am.* **72**, 1479-1492.
- ARVO** (1994). Statement for the use of animals in ophthalmic and vision research. *Invest. Ophthalmol. Vis. Sci.* **35**, v-vi.
- Benedek, G.** (1971). Theory of the transparency of the eye. *Appl. Optics* **10**, 459-473.
- Benedek, G.** (1983). Why the eye lens is transparent. *Nature* **302**, 383-384.
- Bettelheim, F. A. and Siew, E. L.** (1983). Effect of change in concentration upon lens turbidity as predicted by random fluctuation theory. *Biophys. J.* **41**, 29-33.
- Bettelheim, F. A.** (1985). Physical basis of lens transparency. In *The Ocular Lens, Structure, Function and Pathology* (ed. H. Mätsel), pp. 265-300. Marcel Dekker, Inc., New York and Basel.
- Boesch, J. S., Lee, C. and Lindahl, R. G.** (1996). Constitutive expression of class 3 aldehyde dehydrogenase in cultured rat corneal epithelium. *J. Biol. Chem.* **271**, 5150-5157.
- Chew, S. J., Beuerman, R. W., Kaufman, H. E. and McDonald, M. B.** (1995). In vivo confocal microscopy of corneal wound healing after excimer laser photorefractive keratectomy. *CLAO J.* **21**, 273-280.
- Cooper, D. L., Baptist, E. W., Enghild, J. J., Isola, N. R. and Klintworth, G. K.** (1991). Bovine corneal protein 54 K (BCP540 is a homologue of the tumor-associated (class 3) rat aldehyde dehydrogenase (TAT_ALD). *Gene* **98**, 201-207.
- Cooper, D. L., Isola, M. R., Stevenson, K. and Baptist, E. W.** (1992). Members of the ALDH gene family are lens and corneal crystallins. In *Enzymology and Molecular Biology of Carbonyl Metabolism*, vol. 328 (ed. H. Werner, D. W. Crabb and J. G. Flynn), pp. 169-179. Plenum Press, New York.
- Cuthbertson, R. A., Tomarev, S. I. and Piatigorsky, J.** (1992). Taxon-specific recruitment of enzymes as major soluble proteins in the corneal epithelium of three mammals, chicken and squid. *Proc. Nat. Acad. Sci. USA* **89**, 4004-4008.
- de Jong, W. W., Hendriks, W., Mulders, J. W. and Bloemendal, H.** (1989). Evolution of eye lens crystallins: the stress connection. *Trends Biochem. Sci.* **14**, 365-368.
- Delaye, M. and Tardieu, A.** (1983). Short-range order of crystallin proteins accounts for eye lens transparency. *Nature* **302**, 415-418.
- Evces, S. and Lindahl, R.** (1989). Characterization of rat cornea aldehyde dehydrogenase. *Arch. Biochem. Biophys.* **274**, 518-524.
- Farrell, R. A. and McCally, R. L.** (1976). On the interpretation of depth dependent light scattering measurements in normal rabbit corneas. *Exp. Eye Res.* **23**, 69-81.
- Fitzsimmons, T. D., Fagerholm, P., Harfstrand, A. and Schenholm, M.** (1992). Hyaluronic acid in the rabbit corne after excimer laser superficial keratectomy. *Invest. Ophthalmol. Vis. Sci.* **33**, 3011-3016.
- Freund, D. E., McCally, R. L. and Farrell, R. A.** (1986). Effects of fibril orientation on light scattering in the cornea. *J. Opt. Soc. Am. A.* **3**, 1970-1982.
- Gallagher, B. and Maurice, D.** (1977). Striations of light scattering in the corneal stroma. *J. Ultrastruct. Res.* **61**, 100-114.
- Goldman, J. N. and Benedek, G. B.** (1967). The relationship between morphology and transparency in the nonswelling corneal stroma of the shark. *Invest. Ophthalmol. Vis. Sci.* **6**, 574-600.
- Goldman, J. N., Benedek, G. B., Dohlman, C. H. and Kravitt, B.** (1968). Structural alterations affecting transparency in swollen human corneas. *Invest. Ophthalmol. Vis. Sci.* **7**, 501-519.
- Goldman, J. N. and Kuwabara, T.** (1968). Histopathology of corneal edema. *Int. Ophthalm. Clin.* **8**, 561-579.
- Graham, C., Hodin, J. and Wistow, G.** (1996). A retinaldehyde dehydrogenase as a structural protein in a mammalian eye lens. Gene recruitment of beta-crystallin. *J. Biol. Chem.* **271**, 15623-15628.
- Guo, J., Sax, C. M., Piatigorsky, J. and Yu, F. X.** (1997). Heterogenous expression of transketolase in ocular tissues. *Curr. Eye Res.* **16**, 467-474.
- Hennighausen, H., Feldman, S. T., Bille, J. F. and McCulloch, A. D.** (1998). Anterior-posterior strain variation in normally hydrated and swollen rabbit cornea. *Invest. Ophthalmol. Vis. Sci.* **39**, 253-262.
- Holt, W. S. and Kinoshita, J. H.** (1973). The soluble proteins of the bovine cornea. *Invest. Ophthalmol. Vis. Sci.* **12**, 114-126.
- Ichijima, H., Petroll, W. M., Jester, J. V., Barry, P. A., Andrews, P. M., Dai, M. and Cavanagh, H. D.** (1993). In vivo confocal microscopic studies of endothelial wound healing in rabbit cornea. *Cornea* **12**, 369-378.
- Jester, J. V., Petroll, W. M., Garana, R. M., Lemp, M. A. and Cavanagh, H. D.** (1992). Comparison of in vivo and ex vivo cellular structure in rabbit eyes detected by tandem scanning microscopy. *J. Microsc.* **165**, 169-181.
- Jester, J. V., Barry, P. A., Lind, G. J., Petroll, W. M., Garana, R. and Cavanagh, H. D.** (1994). Corneal keratocytes: in situ and in vitro organization of cytoskeletal contractile proteins. *Invest. Ophthalmol. Vis. Sci.* **35**, 730-743.
- Jester, J. V., Petroll, W. M., Barry, P. A. and Cavanagh, H. D.** (1995). Temporal, 3-dimensional, cellular anatomy of corneal wound tissue. *J. Anat.* **186**, 301-311.
- Kaye, G. I.** (1969). Stereologic measurement of cell volume fraction of rabbit corneal stroma. *Arch. Ophthalmol.* **82**, 792-794.
- Kays, W. T. and Piatigorsky, J.** (1997). Aldehyde dehydrogenase class 3 expression: identification of a cornea-preferred gene promoter in transgenic mice. *Proc. Nat. Acad. Sci. USA* **94**, 13594-13599.
- King, G. and Holmes, R. S.** (1998). Human ocular aldehyde dehydrogenase isozymes: Distribution and properties as major soluble proteins in cornea and lens. *J. Exp. Zool.* **282**, 12-17.
- Knoishi, Y. and Mimura, Y.** (1992). Kinetic properties of the bovine corneal aldehyde dehydrogenase (BCP 54). *Exp. Eye Res.* **55**, 569-578.
- Kurzchalia, T. V., Dupree, P., Partin, R. G., Kellner, R., Virta, H., Lehnert, M. and Simons, K.** (1992). VIP21, A 21-kD membrane protein is an integral component of trans-Golgi-network-derived transport vesicles. *J. Cell Biol.* **118**, 1003-1014.
- Li, H.-F., Petroll, W. M., Moller-Pedersen, T., Maurer, J. K., Cavanagh, H. D. and Jester, J. V.** (1997). Epithelial and corneal thickness measurements by in vivo confocal microscope through focusing (CMTF). *Curr. Eye Res.* **16**, 214-221.
- Lindahl, R. and Peterson, D. R.** (1991). Lipid aldehyde oxidation as a physiological role for class 3 aldehyde dehydrogenases. *Biochem. Pharmacol.* **41**, 1583-1587.
- Maurice, D. M.** (1957). The structure and transparency of the cornea. *J. Physiol.* **136**, 263-286.
- Maurice, D. M.** (1962). The Cornea and Sclera. In *The Eye*, vol. 1 (ed. H. Davson), pp. 289-361. Academic Press, New York.
- McCally, R. L. and Farrell, R. A.** (1976). The depth dependence of light scattering from the normal rabbit cornea. *Exp. Eye Res.* **23**, 69-81.
- McCally, R. L. and Farrell, R. A.** (1982). Structural implications of small-angle light scattering from cornea. *Exp. Eye Res.* **34**, 99-113.
- Messiha, F. S. and Price, J.** (1983). Properties and regional distribution of ocular aldehyde dehydrogenase in the rat. *Neurobehav. Toxicol. Teratol.* **5**, 251-254.
- Mitchell, J. and Cenedella, R. J.** (1995). Quantitation of ultraviolet light absorbing fraction of the cornea. *Cornea* **14**, 266-272.
- Moller-Pedersen, T., Vogel, M., Li, H. F., Petroll, W. M., Cavanagh, H. D. and Jester, J. V.** (1997). Quantification of stromal thinning, epithelial

- thickness and corneal haze after photorefractive keratectomy using in vivo confocal microscopy. *Ophthalmology* **104**, 360-368.
- Moller-Pedersen, T., Cavanagh, H. D., Petroll, W. M. and Jester, J. V.** (1998a). Neutralizing antibody to TGF β modulates stromal fibrosis but not regression of photoablative effect following PRK. *Curr. Eye Res.* **17**, 736-747.
- Moller-Pedersen, T., Li, H. F., Petroll, W. M., Cavanagh, H. D. and Jester, J. V.** (1998b). Confocal microscopic characterization of wound repair after photorefractive keratectomy. *Invest. Ophthalmol. Vis. Sci.* **39**, 487-501.
- Montgomery, M. K. and McFall-Ngai, M. J.** (1992). The muscle-derived lens of a squid bioluminescent organ is biochemically convergent with the ocular lens. Evidence for recruitment of aldehyde dehydrogenase as a predominant structural protein. *J. Biol. Chem.* **267**, 20999-21003.
- Muller, L. J., Pels, L. and Vrensen, G. F. J. M.** (1995). Novel aspects of the ultrastructural organization of human corneal keratocytes. *Invest. Ophthalmol. Vis. Sci.* **36**, 2557-2567.
- Petroll, W. M., Cavanagh, H. D. and Jester, J. V.** (1993). Three-dimensional imaging of corneal cells using in vivo confocal microscopy. *J. Microsc.* **170**, 213-219.
- Petroll, W. M., Jester, J. V. and Cavanagh, H. D.** (1996). In vivo confocal imaging. *Int. Rev. Exp. Path.* **36**, 93-129.
- Piatigorsky, J.** (1998). Gene sharing in lens and cornea. Facts and implications. *Prog. Retinal Eye Res.* **17**, 145-174.
- Piatigorsky, J. and Wistow, G.** (1989). Enzyme/crystallin:gene sharing as an evolutionary strategy. *Cell* **57**, 197-199.
- Rabaey, M. and Segers, J.** (1981). Changes in the polypeptide composition of the bovine corneal epithelium during development. In *Cong. Eur. Soc. Ophthalmol.* (ed. P. D. Trevor-Rope), pp. 41-44. Academic Press, London.
- Roza, A. J. and Beuerman, R. W.** (1982). Density and organization of free nerve endings in the corneal epithelium of the rabbit. *Pain* **14**, 105-120.
- Sax, C. M., Salamon, C., Kays, W. T., Guo, J., Yu, F., Cuthbertson, R. A. and Piatigorsky, J.** (1996). Transketolase is a major protein in the mouse cornea. *J. Biol. Chem.* **271**, 33568-33574.
- Silverman, B., Alexander, R. J. and Henley, W. L.** (1981). Tissue and species specificity of BCP 54, the major soluble protein of bovine cornea. *Exp. Eye Res.* **33**, 19-39.
- Tomarev, S. I. and Piatigorsky, J.** (1996). Lens crystallins of invertebrates. Diversity and recruitment from detoxification enzymes and novel proteins. *Eur. J. Biochem.* **235**, 449-465.
- Uma, L., Hariharan, J., Sharma, Y. and Balasubramanian, D.** (1996). Corneal aldehyde dehydrogenase displays antioxidant properties. *Exp. Eye Res.* **63**, 117-120.
- Verhagen, C., Hoekzema, R., Verjans, G. M. G. M. and Kijlstra, A.** (1991). Identification of bovine corneal protein 54 (BCP54) as an aldehyde dehydrogenase. *Exp. Eye Res.* **53**, 283-284.
- Watsky, M. A.** (1995). Keratocyte gap junctional communication in normal and wounded rabbit corneas and human corneas. *Invest. Ophthalmol. Vis. Sci.* **36**, 2568-2576.
- Weber, B. A., Fagerholm, P. and Johansson, B.** (1997). Colocalization of hyaluronan and water in rabbit corneas after photorefractive keratectomy by specific staining for hyaluronan and by quantitative microradiography. *Cornea* **16**, 560-563.
- Wistow, G. J. and Piatigorsky, J.** (1988). Lens crystallins: The evolution and expression of proteins for a highly specialized tissue. *Annu. Rev. Biochem.* **57**, 479-504.
- Wistow, G. and Kin, H.** (1991). Lens protein expression in mammals: taxon-specificity and the recruitment of crystallins. *J. Mol. Evol.* **32**, 262-269.
- Zinovieva, R. D., Tomarev, S. I. and Piatigorsky, J.** (1993). Aldehyde dehydrogenase-derived omega-crystallins of squid and octopus. Specialization for lens expression. *J. Biol. Chem.* **268**, 11449-11455.